Am J Cancer Res 2023;13(4):1310-1328
www.ajcr.us /ISSN:2156-6976/ajcr0147485

Original Article

Guanylate binding protein 5 accelerates gastric cancer progression via the *JAK1-STAT1/GBP5/CXCL8* positive feedback loop

Feng-Yu Cao[1*], Chen-Hong Wang[1*], Xiang Li[1*], Ming-Zhen Ma[1], Gong-Cai Tao[1], Chao Yang[1], Kai Li[1], Xiao-Bo He[1], Shi-Lun Tong[1], Qing-Chuan Zhao[2], Song Su[3], Dan Song[1], Yong-Bin Zheng[1]

[1]Department of Gastrointestinal Surgery, Key Laboratory of Hubei Province for Digestive System Disease, Renmin Hospital of Wuhan University, Wuhan 430000, Hubei, China; [2]State Key Laboratory of Cancer Biology, National Clinical Research Center for Digestive Diseases and Xijing Hospital of Digestive Diseases, Xijing Hospital, Fourth Military Medical University, Xi'an 710032, Shaanxi, China; [3]Department of Gastroenterology, The First Medical Center of Chinese PLA General Hospital, Beijing 100853, China. [*]Equal contributors.

Received November 2, 2022; Accepted March 11, 2023; Epub April 15, 2023; Published April 30, 2023

Abstract: Guanylate binding protein 5 (GBP5) is a member of the interferon (IFN)-inducible large guanosine triphosphate hydrolases (GTPase) family that regulates cell-autonomous immunity and malignant tumor transformation. However, its specific roles and underlying mechanisms GBP5 in gastric cancer (GC) remain unknown. In this study, we aimed to determine the role GBP5 and underlying mechanism of *GBP5* in GC cell progression. Potential oncogenic roles of *GBP5* in GC as well as its relationship with the tumor immune microenvironment (TIME) were comprehensively evaluated using bioinformatics analysis. Protein expression levels of GBP5 and their correlation with clinicopathological features of patients were assessed using immunohistochemistry. In addition, diverse in vitro functional experiments were performed to identify the functions of *GBP5* in GC. Downstream targets of *GBP5* were identified using RNA-sequencing analysis and verified using western blotting or quantitative polymerase chain reaction analysis in different cell lines. *GBP5* expression is commonly upregulated and promotes the proliferation and migration of GC cells. Mechanistically, *GBP5* was regulated by the IFNγ-Janus kinase (JAK1)-signal transducer and activator of transcription 1 (STAT1) axis and induced CXCL8 expression. Interestingly, *GBP5*-induced CXCL8 regulated the *JAK1-STAT1* signaling pathway to form a positive feedback loop. Moreover, *GBP5* is closely related to the TIME and may be used as a biomarker for predicting the efficacy of immunotherapy. Our findings revealed a new *JAK1-STAT1/GBP5/CXCL8* pathway and highlighted the value of *GBP5* as a predictive biomarker and novel target for GC intervention.

Keywords: Gastric cancer, GBP5, CXCL8, IFNγ-JAK1-STAT1 signaling, positive feedback loop

Introduction

Gastric cancer is a serious health problem and the second leading cause of death worldwide [1]. Gastric cancer (GC) is a common digestive system tumor affected by various factors, including gene expression, *Helicobacter pylori infection*, the environment, and diet [2]. Although the incidence of GC has decreased in recent years, the estimated numbers of new GC cases and deaths in 2022 were the third highest in China [3]. Traditional treatments, such as surgery and chemotherapy, have limited effects on improving the patient prognosis. With the development of technology, the treatment of GC is improving with the aid of precision medicine [4]. Therefore, it is necessary to identify genes playing important roles in the development of GC.

The guanylate-binding proteins (GBPs), members of the translation factor (TRAFAC) class dynamin-like GTPase superfamily, are involved in important cellular processes, including signal transduction, gene translation, vesicle trafficking, and exocytosis [5-8]. Among GBP family members, GBP5 is a critical cellular factor in inflammasome assembly that is considered as

a central orchestrator of neoplastic disease immunity [9, 10]. Malignancy-related functions and prognostic value of *GBP5* in tumor progression suggest its potential clinical significance [11-13]. For example, in triple-negative breast cancer, *GBP5* can promote tumor cell migration by inducing programmed death-ligand 1 (*PD-L1*) expression [12]. In addition, *GBP5* is highly expressed in gastric adenocarcinoma and medullary carcinoma [14, 15]. However, the specific role of *GBP5* in GC remains unclear.

CXCL8 contributes to immune suppression in the tumor microenvironment (TME) [16]. It can act in a paracrine manner to alter the composition of immune infiltration in TME [17] by recruiting tumor-associated macrophages [18], myeloid-derived suppressor cells, and tumor-associated neutrophils [19] to the TME and inhibiting the anti-tumor activity of NK cells [20] and dendritic cell migration without impairing T-cell stimulation [21]. Additionally, CXCL8 expression is highly correlated with various immune characteristics, including immune modulator, chemokine, and drug levels, and can act as a prognostic marker for immune therapy response in patients with different cancer types [22-26]. However, the detailed mechanism underlying the regulation of *CXCL8* remains unknown.

In this study, we investigated the biological role of *GBP5* in GC. We found that *GBP5* expression was upregulated and promoted the proliferation and migration of GC cells. *GBP5* expression was regulated by the *IFNγ-JAK1-STAT1* axis and induced CXCL8 expression. We also found that *GBP5*-induced CXCL8 regulated the *JAK1-STAT1* signaling pathway to form a positive feedback loop. In addition, *GBP5* was closely related to the tumor immune microenvironment (TIME) and may be a marker for predicting the efficacy of immunotherapy in patients with GC.

Materials and methods

Cell culture and construction of lentiviral cell lines

Human GC cells (MKN45 and BGC823) were stored in our laboratory and authenticated using STR profiling. Cells were inoculated into Dulbecco's modified Eagle's medium (Grand Island, NY, USA) supplemented with 10% fetal bovine serum, 100 μg/mL Gibco-penicillin, and 100 μg/mL Gibco-streptomycin at 37°C with 5% CO_2. Cells were transfected with overexpression and/or knockdown lentiviral vectors designed and supplied by HANBIO Co. Ltd. (Shanghai, China). *GBP5* knockdown shRNA sequence was GATGATGAGCTAGAGCCTGAA. Multiplicity of infection of transfection was approximately 50. Cells were treated with 2 μg/mL puromycin for 1 week 72 h after infection.

Tumor samples

Tissue microarray (TMA) was obtained from the State Key Laboratory of Cancer Biology, National Clinical Research Center for Digestive Diseases, Xijing Hospital, Fourth Military Medical University (Xi'an, China). TMA contained 170 gastric tumor and paired adjacent non-tumor tissue samples and was used to determine *GBP5* expression levels in GC and matched normal tissues. Patient clinical characteristics, including patient age, gender, tumor location, and TNM stage, are presented in **Table 1**. This study was approved by the Xijing Hospital Protection of Human Subjects Committee. All participants provided informed consent prior to their participation in this study.

RNA extraction and reverse transcription-quantitative polymerase chain reaction (RT-qPCR)

Total RNA was extracted from the cells using the TaKaRa MiniBEST Universal RNA Extraction Kit (Cat# 9767, Takara, Japan), and cDNA was synthesized using a Takara-reverse transcription kit (Cat# RR036A, Japan). Subsequently, the Takara-SYBR Green PCR Kit (Cat# RR820A, Japan) was used to perform RT-qPCR on a Bio-Rad CFX96 system (CA, USA) using the following program: pre-denaturation at 95°C for 10 min, 40 cycles of denaturation at 95°C for 15 s, primer annealing at 60°C for 1 min, and final elongation at 72°C for 30 s. Fluorescence was measured and Ct values were calculated using Applied Biosystems-SDS 1.9.1 software. The reactions were performed in triplicates. The sequences of the primers were as follows: *GBP5*-F, CTGTCTGCCATTACGCAACCTG; *GBP5*-R, GTGTGAGACTGCACCGTAGATG.

Western blotting analysis

Proteins were extracted from cultured cells using radioimmunoprecipitation assay buffer

Table 1. Correlation between the Guanylate binding protein 5 (*GBP5*) expression levels in tissues and clinicopathological characteristics of patients with gastric cancer (GC)

Variables	Cases (No.) (n=170)	GBP5		*P* value
		Low	High	
Age (years)				0.914
< 60 (%)	97	38	59	
≥ 60 (%)	73	28	45	
Gender				0.850
Male (%)	125	48	77	
Female (%)	45	18	27	
Tumor Location				0.123
1 upper	34	8	26	
2 middle	65	28	37	
3 low	71	30	41	
Tumor size				0.255
< 5 (%)	71	24	47	
≥ 5 (%)	99	42	57	
Invading surrounding organ tissues				0.634
0	128	51	77	
1	42	15	27	
Lymphatic enlargement				0.726
0	108	43	65	
1	62	23	39	
lymphatic metastasis				0.427
0	28	9	19	
1	142	57	85	
Vascular invasion				0.707
0	70	26	44	
1	100	40	60	
T stage				0.410
T1	15	6	9	
T2	27	10	17	
T3	104	37	67	
T4	24	13	11	
N stage				0.017
N0	28	9	19	
N1	47	12	35	
N2	45	17	28	
N3	50	28	22	
Metastasis				0.844
0	167	65	102	
1	3	1	2	
TNM				0.422
1	26	8	18	
2	49	16	33	
3	92	41	51	
4	3	1	2	
Histological differentiation				0.035
1	95	42	53	
2	39	8	31	
3	17	7	10	

supplemented with a cocktail of Millipore protease and phosphatase inhibitors. Denatured proteins were resolved on a 10% SDS-PAGE gel for immunoblotting analysis with the indicated antibodies. Protein bands were visualized and quantified as previously described [27].

Immunohistochemistry (IHC)

TMA on glass slides were placed in an incubator at 60°C for 1 h, deparaffinized in xylene, rehydrated through graded ethanol solutions, and subjected to antigen retrieval in boiling citrate buffer (0.01 M, pH 6.0) for 2 min. After washing thrice with phosphate-buffered saline (pH 7.5) for 5 min each time, the microarray was treated with 3% hydrogen peroxide solution in methanol for 10 min to quench endogenous peroxidase activity, followed by preincubation with 5% goat serum for 30 min at room temperature to block nonspecific binding. Slides were then incubated at 4°C overnight with GBP5 antibody in blocking buffer. After washing, the tissue sections were treated with peroxidase-labelled polymer conjugated to goat anti-rabbit or anti-mouse immunoglobulin for 30 min at room temperature (25°C). After visualizing the immunostaining with diaminobenzidine tetrahydrochloride (DAB), the sections were counterstained with hematoxylin, dehydrated, and covered with coverslips. Immunohistochemical staining results for each section were calculated as previously described [27]. Briefly, the IHC score for each TMA was calculated by multiplying the staining intensity in four grades (0, negative; 1, weakly positive; 2, moderately positive; 3, strongly positive) by the per-

centage of positive cells in four grades (1, less than 25%; 2, 25-50%; 3, 0-75%; 4, 75-100%).

5-ethynyl-20-deoxyuridine incorporation and colony formation assays

MKN45 and BGC823 cells were cultured in 96-well plates. At 37°C, cells were treated with 50 μM 5-ethynyl-20-deoxyuridine (EdU, Ribobio, China) for 2 h. Then, cells were fixed with formaldehyde for 30 min and treated with 0.5% Triton X-100 for 10 min. Next, 100 μl of the 1 × Apollo reaction cocktail was added to each well for 30 min. Finally, the cells with 100 μl of 1 × Hoechst 33,342 for 30 min and observed under a fluorescence microscope. For colony formation assays, MKN45 and BGC823 cells were seeded at a density of 2,000 cells/well in 6-well plates. The cells were cultured for 2 weeks, during which the culture medium was changed once every 3 days. The number of colonies in each well was counted.

In vitro cell migration assay

An 8-μm pore 24-well Corning Transwell plate (MA, USA) was employed to assay the migration potential of all cell lines. We coated the chamber inserts with an 8-μm pore size, and the upper compartment was inoculated with 6 × 10^4 cells suspended in serum-free media, and 20% FBS was employed as a chemo-attractant and applied to the lower chamber. The cells were allowed to grow at 37°C for a specified time period, followed by fixation with 4% paraformaldehyde. Crystal violet staining was performed and the cells at × 100 under a microscope (Olympus, Tokyo, Japan). All assays were performed in triplicates. The degree of migration was determined as the ratio of the number of treated cells to that of control cells.

Transcriptomic analysis

RNA-Seq transcriptome analysis was performed in *GBP5*-overexpressed MKN45 and control cells to assess the changes in global gene expression. Differentially expressed genes (DEGs) between high and low *GBP5* expression groups were identified, where |log2-fold change (FC)| > 1 and $P < 0.05$ were set as the cutoff values. Gene Ontology (GO) and Kyoto Encyclopedia of Genes and Genomes (KEGG) pathway enrichment analyses were conducted to interpret the functions of differentially expressed genes. The differentially expressed proteins were uploaded to Search Tool for the Retrieval of Interacting Genes/Proteins (https://string-db.org) to construct protein-protein interaction (PPI) networks. Gene set enrichment analysis (GSEA; using the Molecular Signatures Database, h.all.v6.0. symbols.gmt) was used to identify the potential function of GBP5.

Bioinformatics analysis

Association between *GBP5* expression and TIME in GC was evaluated using bioinformatic methods. First, GC samples from The Cancer Genome Atlas (TCGA) were divided into hot and cold tumors based on the degree of CD8A expression. Specifically, CD8A expression in the top 10% of GC and bottom 10% were defined as hot and cold tumors, respectively. Expression differences of GBP5 between cold and hot tumors were compared, and the immune-related genes associated with GBP5 were analyzed. In addition, the correlations between GBP5 expression and immune score, stroma score, tumor purity, and the Estimation of STromal and Immune cells in MAlignant Tumor tissues using Expression data (ESTIMATE) score of GC samples were evaluated. Moreover, the Cell-type Identification by Estimating Relative Subsets of RNA Transcripts (CIBERSORT) and Tumor Immune Estimation Resource (TIMER) methods were used to determine the degree of immune cell infiltration [28, 29].

Quantification and statistical analysis

SPSS (V.19.0) and Prism version 9.0 and 4.1.1 version R were used to conduct the data analysis. Fisher's exact test was used to analyze the categorical data. Student's t-test or Wilcoxon test was used for intergroup comparisons of quantitative data. Kaplan-Meier survival analysis and log-rank test were used to explore cumulative survival rates. To identify the indicators that independently affected survival, predetermined variables established to be significant were subjected to multivariate analysis and further analyzed using the Cox proportional hazards model. Pearson's coefficient was used to explore the correlation between variables. Statistical significance was set at $P < 0.05$.

Results

GBP5 is significantly overexpressed in patients with GC

To investigate the expression of GBP5 in GC, we first analyzed the expression of GBP5 online through the Gene Expression Profiling Interactive Analysis (GEPIA) website based on The Cancer Genome Atlas (TCGA) and Genotype-Tissue Expression datasets, and found that it was significantly overexpressed in GC (**Figure 1A**) [30]. Moreover, Kaplan-Meier analysis showed that patients with higher GBP5 levels had shorter overall survival (**Figure 1B**) [31]. We aimed to clarify whether gene mutations play a role in GBP5 dysregulation. We evaluated the genetic alterations of GBP5 in patients with GC using the cBio Cancer Genomics Portal (cBioPortal) database [32]. Seven datasets of GC were used, including Gastric Cancer (OncoSG, 2018), Stomach Adenocarcinoma (Pfizer and UHK, Nat Genet 2014), Stomach Adenocarcinoma (TCGA, Firehose Legacy), Stomach Adenocarcinoma (TCGA, Nature 2014), Stomach Adenocarcinoma (TCGA, PanCancer Atlas), Stomach Adenocarcinoma (U Tokyo, Nat Genet 2014), and Stomach Adenocarcinoma (UHK, Nat Genet 2011) were analyzed. Among the datasets analyzed, the frequency of gene alterations, including mutations, amplification, and deep deletions, was up to 3%, with mutations being the most commonly observed alteration (**Figure 1C**). **Figure 1D** summarizes the correlation between alterations and clinical characteristics of patients with GC.

We also analyzed GBP5 expression in four tissue micro-arrays containing 170 paired GC specimens by IHC analysis. The data showed that GBP5 was predominantly distributed GBP5 in the nucleus and cytoplasm of GC cells. **Figure 1E** shows GBP5 IHC staining trends in GC. Statistical analysis further confirmed that GBP5 protein levels were significantly higher in GC tissues than in the adjacent non-malignant tissues (**Figure 1F**). In addition, GBP5 protein expression was further analyzed using our previously reported proteomics data, which adopted 48 paired laser capture microdissection cancer tissues that were histologically classified as signet ring cell carcinoma (n=14), poorly differentiated adenocarcinoma (n=17), and well-moderately differentiated adenocarcinoma (n=17) [33]. The results showed that GBP5 was commonly upregulated in patients with the three subtypes (**Figure 1G**). Taken together, GBP5 was overexpressed in GC, indicating that GBP5 may play a critical role in GC development.

Next, we determined the relationship between GBP5 expression and clinicopathological characteristics of 170 GC tissue samples with available associated clinical details. GBP5 was highly expressed in 61.1% (104/170) of the GC tissues (**Table 1**). There were no significant associations between GBP5 expression and patient age, gender, vascular invasion, tumor size, lymphatic enlargement, metastasis, or TNM stage. However, GBP5 expression correlated with N stage (P=0.017) and histological differentiation (P=0.035). In addition, we used univariate and multivariate analyses of various factors associated with overall survival in patients with GC. Univariate analysis showed that gender, tumor size, invasion of surrounding organ tissues, lymphatic enlargement, lymph node metastasis, vascular invasion, and TNM stage were significantly correlated with patient survival (**Table 2**). Multivariate analysis suggested a positive correlation among gender, lymphatic enlargement, and prognosis.

GBP5 promotes GC cell proliferation and migration in vitro

To investigate whether GBP5 manipulates the biological behavior of GC cells, we utilized three independent short hairpin RNAs (shRNAs) sh-NC, sh-GBP5-1, sh-GBP5-2, and sh-GBP5-3 to knockdown GBP5 expression in the GC cell line (BGC823) with higher basal expression and overexpressed GBP5 expression in the cell line (MKN45) with lower basal expression of GBP5 (**Figure 2A**). However, at the protein level, GBP5 showed only a slight silencing effect when using sh-GBP5-1 and sh-GBP5-3 compared to sh-GBP5-2. Based on these results, shGBP5-2 was selected for the subsequent experiments. Quantitative real-time PCR (RT-qPCR) were performed to evaluate transfection efficiency (**Figure 2B**). Based on the results above, we carried out EdU, colony formation, and transwell assays to evaluate the proliferation and migration ability of GC cell lines. We found that GBP5-knockdown distinctly impairs the viabili-

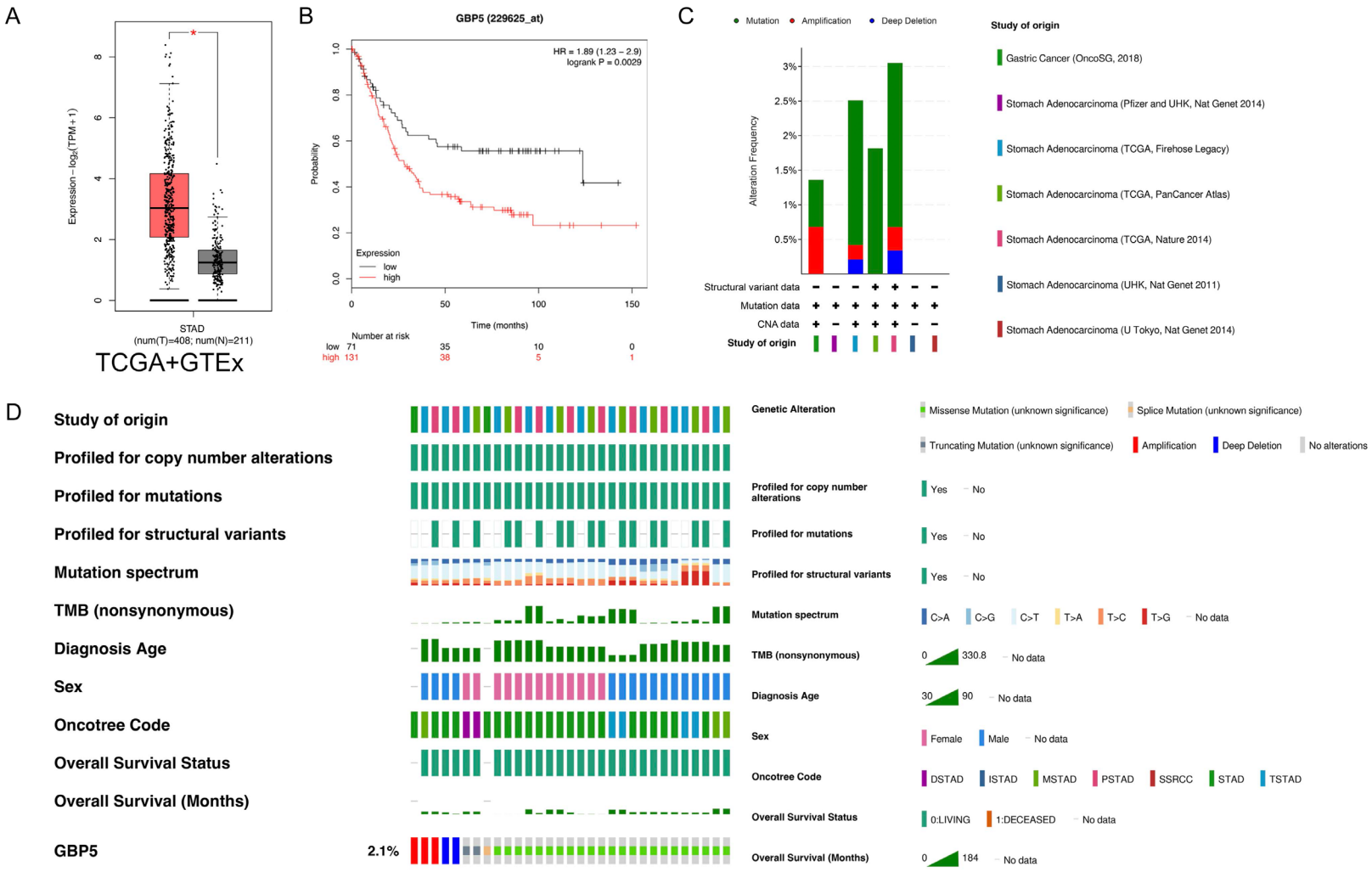
A
Expression − log2(TPM + 1)
STAD
(num(T)=408; num(N)=211)
TCGA+GTEx
B
GBP5 (229625_at)
HR = 1.89 (1.23 − 2.9)
logrank P = 0.0029
Probability
Expression
low
high
Time (months)
Number at risk
low 71 35 10 0
high 131 38 5 1
C
Mutation
Amplification
Deep Deletion
Alteration Frequency
Structural variant data
Mutation data
CNA data
Study of origin
Study of origin
Gastric Cancer (OncoSG, 2018)
Stomach Adenocarcinoma (Pfizer and UHK, Nat Genet 2014)
Stomach Adenocarcinoma (TCGA, Firehose Legacy)
Stomach Adenocarcinoma (TCGA, PanCancer Atlas)
Stomach Adenocarcinoma (TCGA, Nature 2014)
Stomach Adenocarcinoma (UHK, Nat Genet 2011)
Stomach Adenocarcinoma (U Tokyo, Nat Genet 2014)
D
Study of origin
Profiled for copy number alterations
Profiled for mutations
Profiled for structural variants
Mutation spectrum
TMB (nonsynonymous)
Diagnosis Age
Sex
Oncotree Code
Overall Survival Status
Overall Survival (Months)
GBP5
2.1%
Genetic Alteration
Missense Mutation (unknown significance)
Splice Mutation (unknown significance)
Truncating Mutation (unknown significance)
Amplification
Deep Deletion
No alterations
Profiled for copy number alterations
Yes
No
Profiled for mutations
Yes
No
Profiled for structural variants
Yes
No
Mutation spectrum
C>A
C>G
C>T
T>A
T>C
T>G
No data
TMB (nonsynonymous)
0
330.8
No data
Diagnosis Age
30
90
No data
Sex
Female
Male
No data
Oncotree Code
DSTAD
ISTAD
MSTAD
PSTAD
SSRCC
STAD
TSTAD
Overall Survival Status
0:LIVING
1:DECEASED
No data
Overall Survival (Months)
0
184
No data

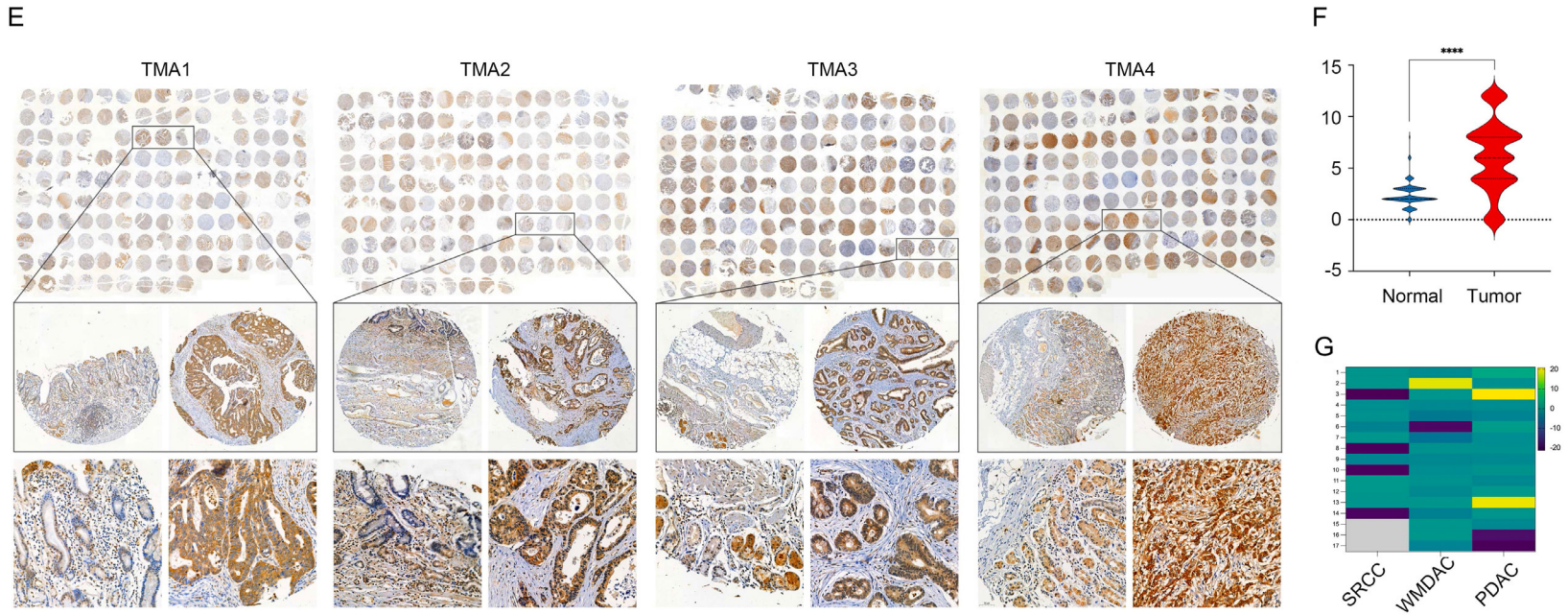

Figure 1. Guanylate binding protein 5 (*GBP5*) expression is significantly upregulated in gastric cancer (GC). (A) Expression levels of *GBP5* in The Cancer Genome Atlas (TCGA) and Genotype-Tissue Expression (GTEX) stomach adenocarcinoma (STAD) datasets. (B) High *GBP5* expression was significantly associated with a short overall survival (OS) (Log-rank test using the Kaplan-Meier Plotter online tools). (C) Alteration frequency of *GBP5* in GC was studied using the cBioPortal. Alteration types included mutations (green), amplifications (red), and deep deletions (blue). (D) Summary of all alterations. In this graphical summary, individual cases are represented as columns. (E, F) Immunohistochemistry (IHC) evaluation (E) and statistical analysis (F) of GC and non-malignant neighboring tissues in tissue micro-arrays (TMAs). (G) GBP5 protein expression levels in proteomics data derived from 48 paired laser capture microdissection (LCM) GC tissues of signet ring cell carcinoma (SRCC; 14 cases), poorly differentiated adenocarcinoma (PDAC; 17 cases) and well-moderately differentiated adenocarcinoma (WMDAC; 17 cases).

Table 2. Univariate and multivariate analyses of factors associated with the overall survival of patients with GC

Variables	OS		
Univariate analysis	*p*	Hazard Ratio	95% confidence interval
Gender	0.001	0.391	0.225-0.677
Tumor size	< 0.001	3.392	2.149-5.352
Invading surrounding organ tissues	< 0.001	2.502	1.642-3.812
Lymphatic enlargement	0.001	1.923	1.294-2.857
Lymphatic metastasis	0.001	3.79	1.755-8.185
Vascular invasion	< 0.001	2.419	1.553-3.770
T classification	< 0.001	2.233	1.668-2.988
N classification	< 0.001	1.884	1.533-2.315
Metastasis	0.003	5.935	1.843-19.110
TNM stage	< 0.001	3.098	2.189-4.384
Age	0.347	0.825	0.553-1.231
Tumor location	0.507	0.918	0.714-1.181
Histological differentiation	0.234	0.828	0.607-1.130
GBP5	0.230	0.784	0.527-1.167
multivariate analysis			
Gender	0.019	0.499	0.278-0.893
Tumor size	0.183	1.452	0.839-2.516
Invading surrounding organ tissues	0.794	1.071	0.640-1.793
Lymphatic enlargement	0.040	1.616	1.023-2.552
Lymphatic metastasis	0.104	0.413	0.142-1.199
Vascular invasion	0.167	1.407	0.867-2.281
T classification	0.071	1.511	0.965-2.366
N classification	0.146	1.355	0.899-2.042
Metastasis	0.288	2.499	0.462-13.525
TNM stage	0.281	1.552	0.698-3.452

ty, DNA replication, and migration abilities of GC cells, whereas overexpression of GBP5 exhibited a contrasting trend (**Figure 2C**, **2D**). Consistent with the results above, the knockdown of GBP5 dramatically increased the ratio of apoptotic cells (**Figure 2E**) and arrested the growth of MKN45 and BGC823 cells in the G0/G1 phase based on flow cytometric assays of apoptosis and cell cycle (**Figure 2F**). Taken together, these data implied that GBP5 plays a pivotal role in the proliferation and migration of GC cells.

GBP5 expression is stimulated by IFNγ in a JAK1-STAT1 axis-dependent manner

The cytokine IFNγ plays an important role in the development of immune cells with anti-tumor activities and immunoediting. Janus (JAK)-signal transduction and activator of transcription (STAT) signaling pathways respond to the IFNγ signaling cascade and are involved in cellular biological processes and immune functions. However, the roles of IFNγ and *JAK1-STAT1* response genes in cancer development are still not completely understood. According to previous studies, GBPs are possibly the most abundantly induced genes upon IFNγ stimulation [5]. Thus, we speculated that GBP5 might be involved in the reactivity of GC cells to IFNγ stimulation by responding to the *JAK1-STAT1* signaling pathway. Therefore, we assessed GBP5 expression in GC cell lines with and without IFNγ stimulation. Changes in STAT1 and phosphorylated STAT1 (p-STAT1), JAK1, and phosphorylated JAK1 (p-JAK1) in this pathway were also analyzed. WB assays indicated that upon stimulation with IFNγ, the signaling pathway was activated, and the expression level of GBP5 in GC cells was significantly increased (**Figure 3A**). To further confirm that the *JAK1-STAT1* signaling pathway mediates the impact of IFNγ induction on GBP5, we developed a combination treatment comprising IFNγ with Fludarabine, a *JAK1/STAT1* Pathway Inhibitor. After treating cells with IFNγ and/or fludarabine, we measured the expression level of GBP5. The results showed that IFNγ alone could upregulate GBP5 expression, but when fludarabine was combined, the effect was offset due to inactivation of the *JAK1-STAT1* signaling pathway (**Figure 3B**). RT-qPCR revealed that IFNγ stimulation affected GBP5 mRNA levels, regardless of the presence of fludarabine (**Figure 3C**). The data indicated that GBP5 expression was stimulated by IFNγ in a *JAK1-STAT1* axis-dependent manner.

Identification of GBP5 downstream targets in GC cells

To verify the role of GBP5 in GC progression, RNA-Seq transcriptome analysis was per-

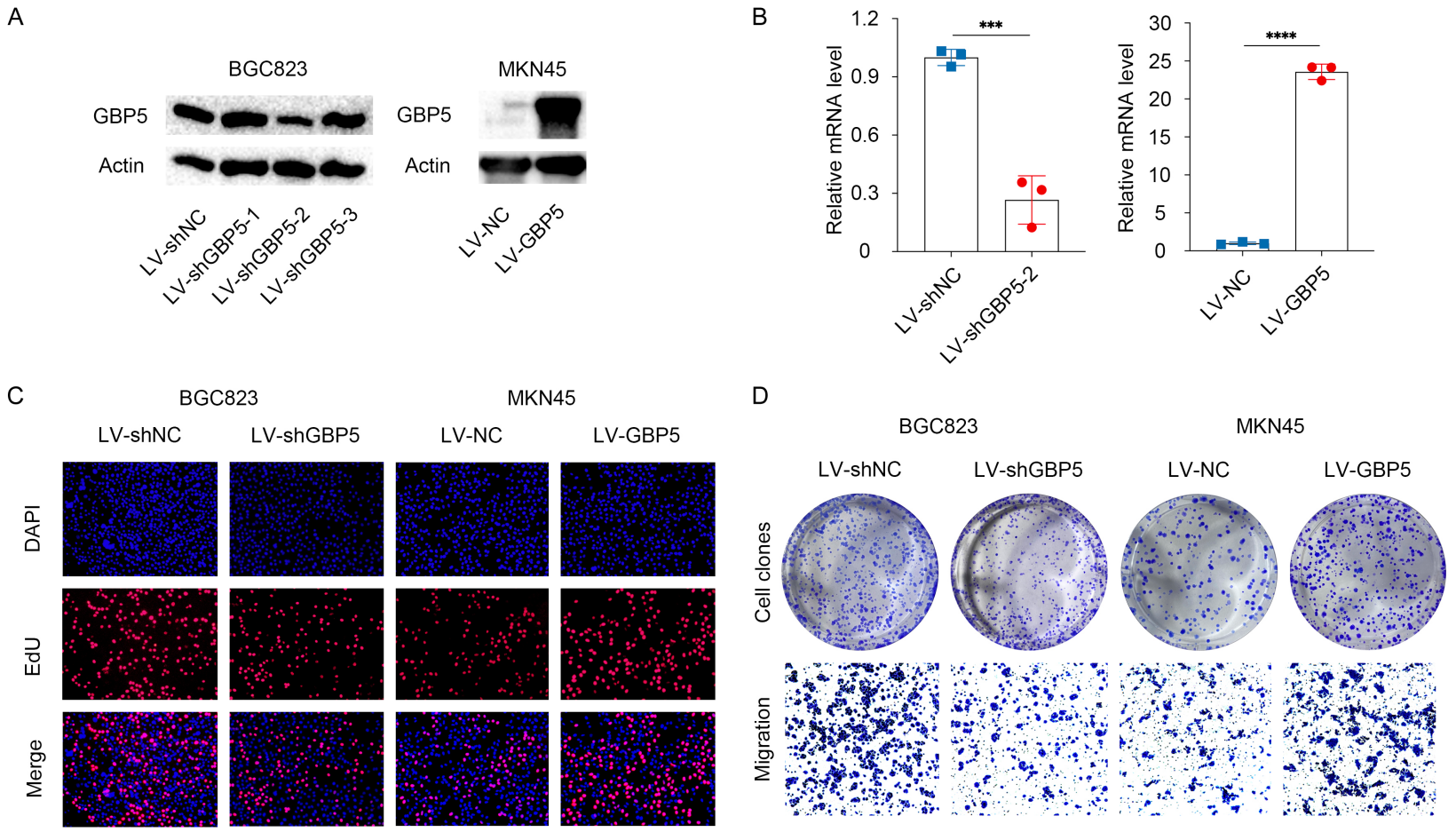
A
BGC823
MKN45
GBP5
Actin
LV-shNC
LV-shGBP5-1
LV-shGBP5-2
LV-shGBP5-3
LV-NC
LV-GBP5
B
Relative mRNA level
1.2
0.9
0.6
0.3
0
***
LV-shNC
LV-shGBP5-2
30
25
20
15
10
5
0
****
LV-NC
LV-GBP5
C
BGC823
MKN45
LV-shNC
LV-shGBP5
LV-NC
LV-GBP5
DAPI
EdU
Merge
D
BGC823
MKN45
LV-shNC
LV-shGBP5
LV-NC
LV-GBP5
Cell clones
Migration

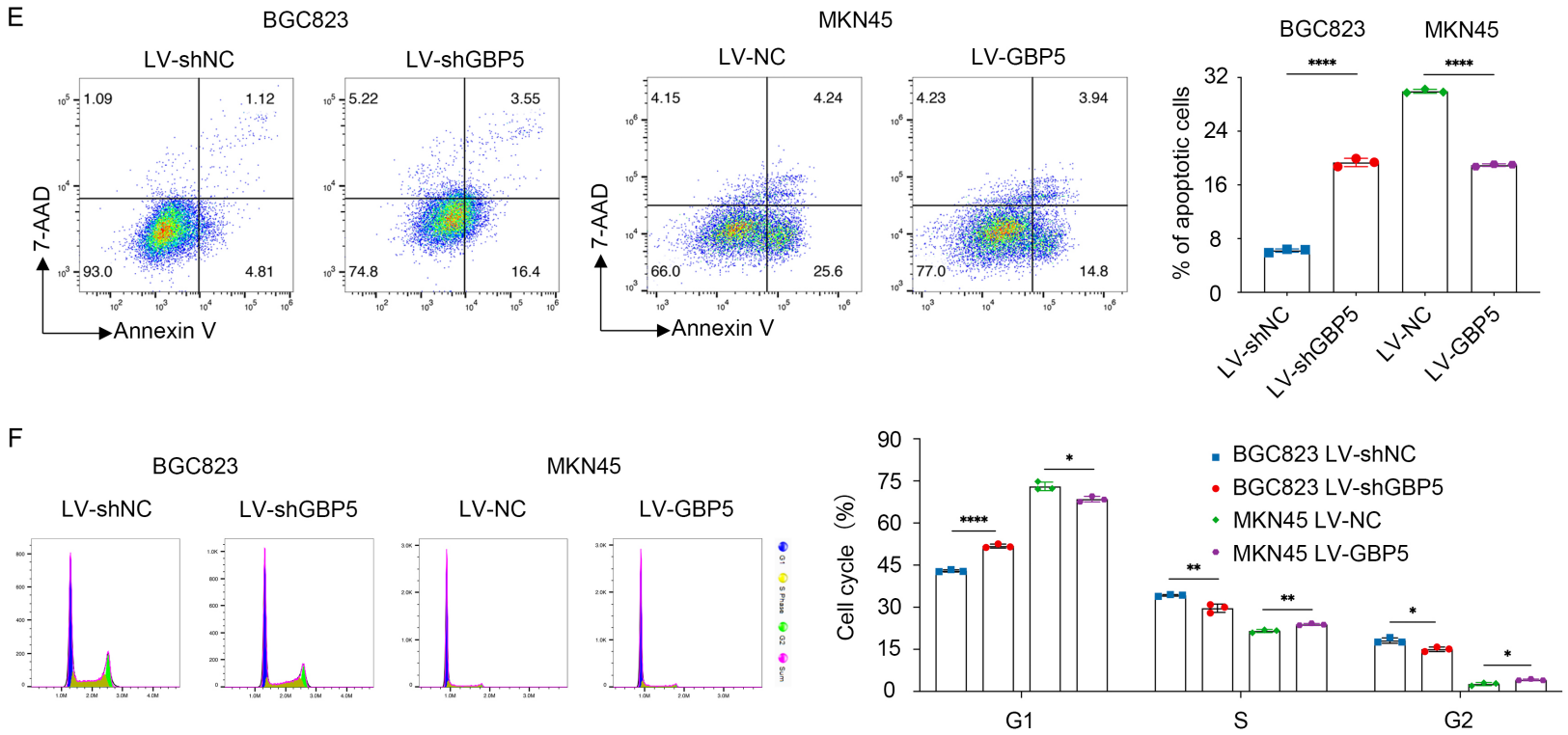

Figure 2. *GBP5* impairs the viability, DNA replication, and migration abilities of GC cells. A. Knockdown of *GBP5* in BGC823 cells and overexpression of *GBP5* in MKN45 cells were confirmed via western blotting. B. Short hairpin RNA (shRNA)-mediated *GBP5* repression and *GBP5* overexpression confirmed via quantitative polymerase chain reaction (RT-qPCR) assay after lentivirus infection in BGC823 and MKN45 cells. C. Proliferation of GC cells with *GBP5* knockdown or overexpression examined via 5-ethynyl-2'-deoxyuridine (EdU) assay. D. Colony-formation and transwell assays to assess the effects of *GBP5* knockdown or overexpression on cell proliferation and migration of GC cells. E. BGC823 and MKN45 cells were stained with annexin V and 7-AAD and analyzed using flow cytometry to assess the effects of *GBP5* knockdown or overexpression on cell apoptosis. F. Effects of *GBP5* knockdown or overexpression on cell cycle progression in BGC823 and MKN45 cells analyzed via flow cytometry. Dip G1, Dip S, and Dip G2 populations are presented (n=3).

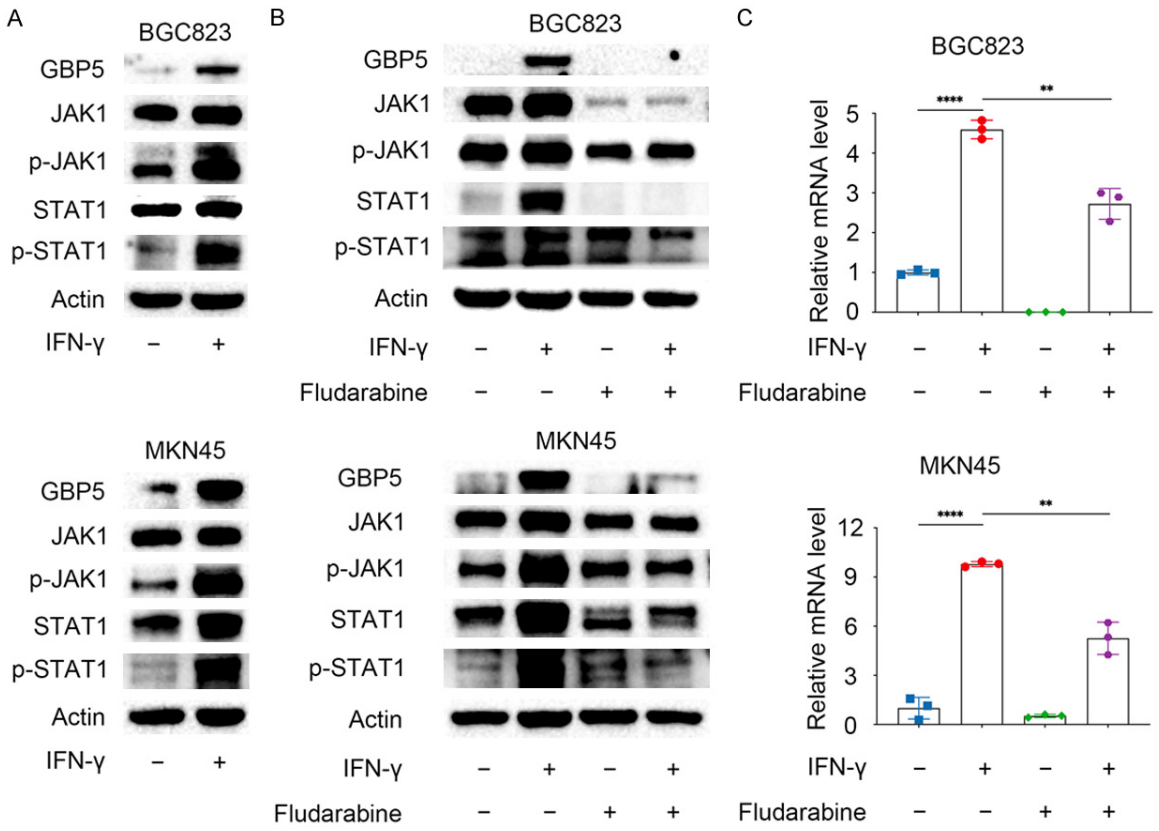

Figure 3. *GBP5* is stimulated by interferon IFNγ in a Janus kinase 1 (JAK1)-signal transducer and activator of transcription 1 (STAT1) axis-dependent manner. A. Effects of IFNγ on STAT1, p-STAT1, JAK1, p-JAK1, and GBP5 expression levels in GC cells determined via western blotting. B. Protein levels of STAT1, p-STAT1, JAK1, p-JAK1, and GBP5 in GC cells treated with IFNγ with or without fludarabine, a STAT pathway-specific inhibitor, determined via western blotting. C. mRNA levels of *GBP5* in GC cells treated with IFNγ with or without fludarabine determined via RT-qPCR.

formed in GBP5-overexpressed MKN45 cells and control cells to assess changes in global gene expression. Differentially expressed genes (DEGs) between the high and low GBP5 groups were identified, where fold change (FC) > 2 and $P < 0.05$, were set as the cutoff values (**Figure 4A**, **4B**, Table S1). The DEGs were significantly enriched in gene sets involved in NF-kappa B signaling pathway, cytokine-cytokine receptor interaction, and JAK1-STAT1 signaling pathway after GBP5 overexpression (**Figure 4C**). Thereafter, we used the gene ontology (GO) database for enrichment analysis to identify the GO terms in which the upregulated genes were significantly enriched. As shown in **Figure 4D**, the DEGs were principally enriched in the inflammatory response. Moreover, KEGG analysis suggested that the upregulated genes were mainly involved in cytokine-cytokine receptor interactions (**Figure 4E**). Next, protein-protein interaction (PPI) networks of the top 30 proteins were constructed (**Figure 4F**). To further identify the potential function of GBP5, GSEA was conducted, and the results showed that substantial gene sets were positively enriched in the GBP5 high-expression group, including inflammatory response (NES=2.08, FDR=0.025), cell response to interferon-gamma (NES=2.05, FDR=0.032), interferon-gamma-mediated signaling pathway (NES=2.15, FDR=0.01), chemokine activity (NES=2.04, FDR=0.028), and cytokine-mediated signaling pathway (NES=2.19, FDR=0.004) (**Figure 4G**). Taken together, these results suggest that GBP5 may promote tumor progression by regulating cytokine-mediated signaling pathways, especially interferon gamma.

CXCL8 is a potential regulatory target of GBP5

The focus now forwards the identification of downstream regulators of GBP5 in cytokine-

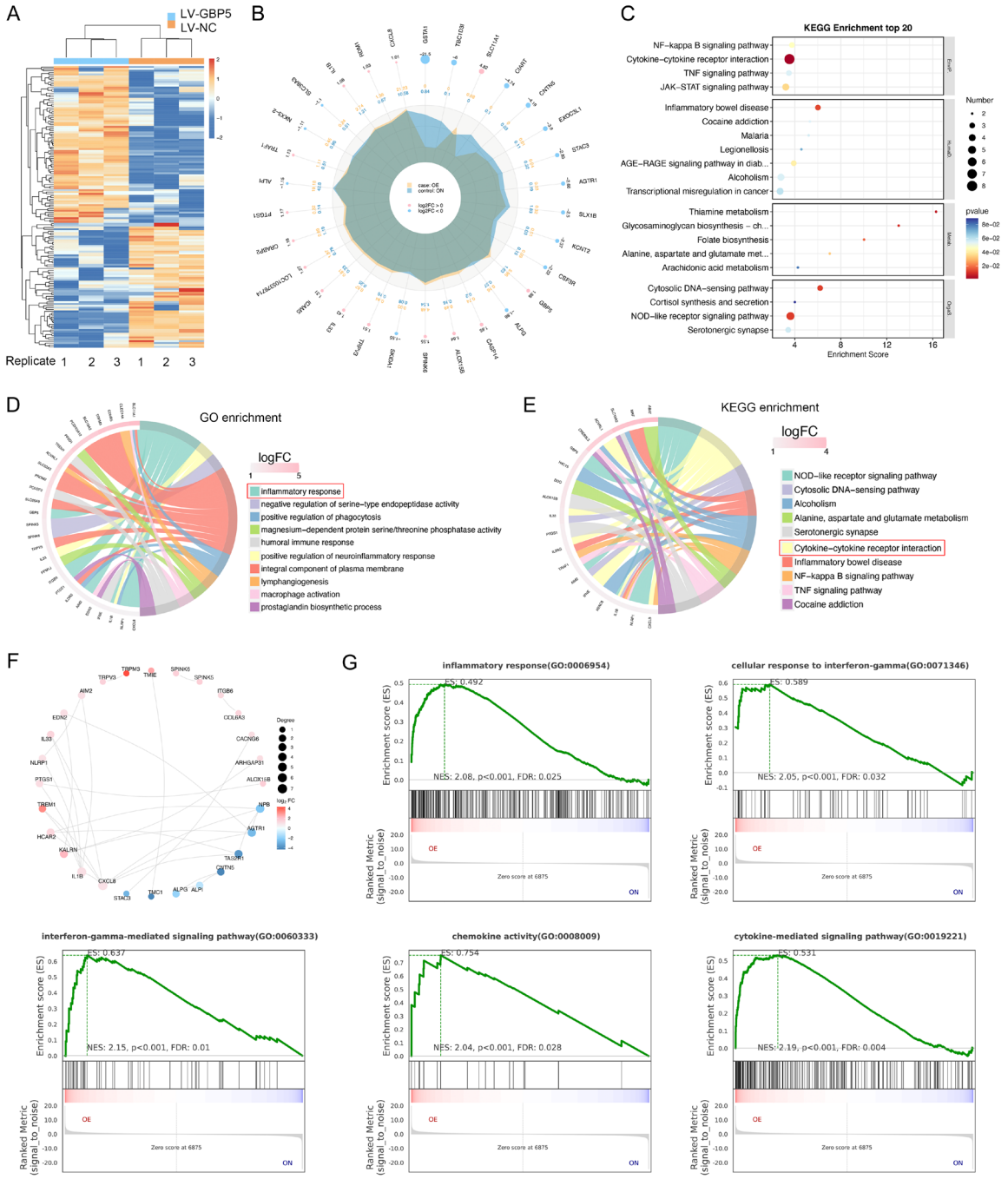

Figure 4. Identification of *GBP5* downstream targets. A. Heatmap of *GBP5* downstream targets assessed via RNA-sequencing (RNA-seq) analysis. Red indicates the upregulated genes, while blue indicates the downregulated genes. B. Upregulated genes based on RNA-seq results. C. Bubble plot of Kyoto Encyclopedia of Genes and Genomes (KEGG) enrichment terms based on RNA-seq results. Alteration in color from red to blue illustrates a decrease in the *P*-value, while the size of the circles indicates the number of genes enriched in KEGG terms. D. Upregulated genes enriched terms of Gene Ontology (GO) analysis. E. Upregulated genes enriched pathways of KEGG analysis. F. Protein-protein interaction (PPI) networks of differentially expressed proteins (DEPs) constructed using the Search Tool for the Retrieval of Interacting Genes/Proteins (STRING) database. Node size is positively associated with the degree of interaction and gradation of color is positively associated with the expression level of this gene. G. Gene set enrichment analysis (GSEA) revealed that inflammatory response, cell response to interferon-gamma, interferon-gamma-mediated signaling pathway, chemokine activity, and cytokine-mediated signaling pathway were positively enriched in GBP5 high-expression group.

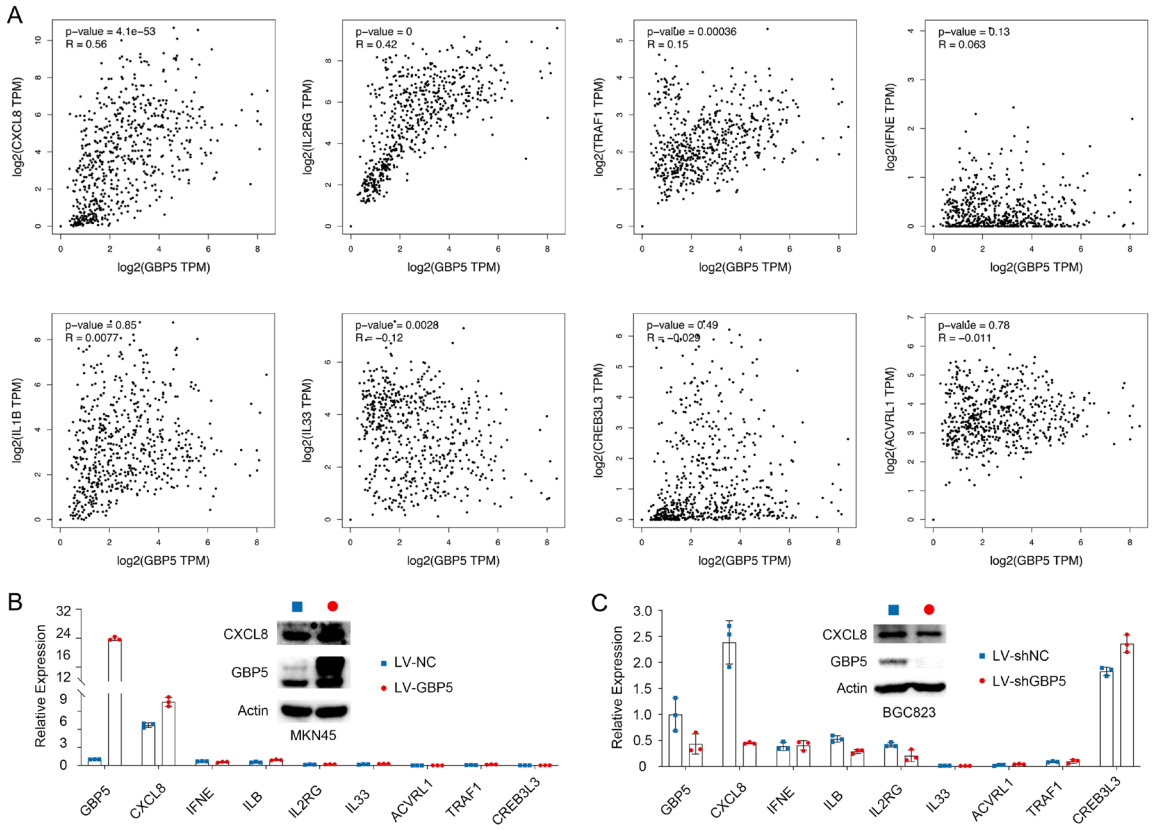

Figure 5. CXCL8 is a potential regulatory target of *GBP5*. (A) Correlation analysis of *GBP5* and different gene mRNA expression levels in the Gene Expression Profiling Interactive Analysis (GEPIA) database. (B, C) RT-qPCR detects the gene expression difference at mRNA level and western blotting detects the correlation between GBP5 and CXCL8 expression at the protein level in MKN45-LV-GBP5 cells (B) and BGC823-LV-shGBP5 cells (C).

cytokine receptor interactions. We first analyzed the correlation between GBP5 and candidate gene mRNA expression using the GEPIA public database. Correlation analysis showed that both CXCL8 and IL2RG had high correlation coefficients with GBP5 expression (**Figure 5A**). Then, mRNA and protein expression levels of some or all of these genes were detected by RT-qPCR and WB to confirm the role of GBP5 in the regulation of expression in MKN45-LV-GBP5 and BGC823-LV-shGBP5 cells. It can be observed that as GBP5 increases, the expression level of CXCL8 increases as well (**Figure 5B**). Similarly, a concomitant decrease in CXCL8 expression was observed when GBP5 was silenced (**Figure 5C**). The consistent trend of changes suggests that CXCL8 may function downstream of GBP5.

Reciprocal positive regulation between GBP5 and CXCL8-JAK1/STAT1 signaling

C-X-C motif ligand 8 (CXCL8) is a chemokine that acts as an important multifunctional cytokine that modulates tumor proliferation, invasion, and migration in an autocrine or paracrine manner. The function of CXCL8 in tumorigenesis and tumor progression relies mainly on chemokine receptor 1 (CXCR1) and CX-C chemokine receptor 2 (CXCR2). Studies have suggested that increased CXCL8 levels indicate poor clinical outcomes and tumor progression in patients with gastric cancer [34]. Therefore, we examined whether CXCL8 functions as a major downstream effector of GBP5 in the stimulation of IFNγ in GC cells. As indicated in **Figure 6A**, the levels of tyrosine-phosphorylated JAK1 and STAT1 were dramatically increased by stimulation with IFNγ compared to those in unstimulated cells. More importantly, CXCL8 trends were consistent with GBP5 trends in IFNγ-treated cells (**Figure 6A**). To further verify that GBP5 regulates the expression of CXCL8-JAK1/STAT1, we used WB to detect changes in the expression of MKN45-LV-GBP5. CXCL8 overexpression was associated with GBP5 overexpression, in accordance with p-JAK1 and p-STAT1 (**Figure 6B**). Next, to examine whether

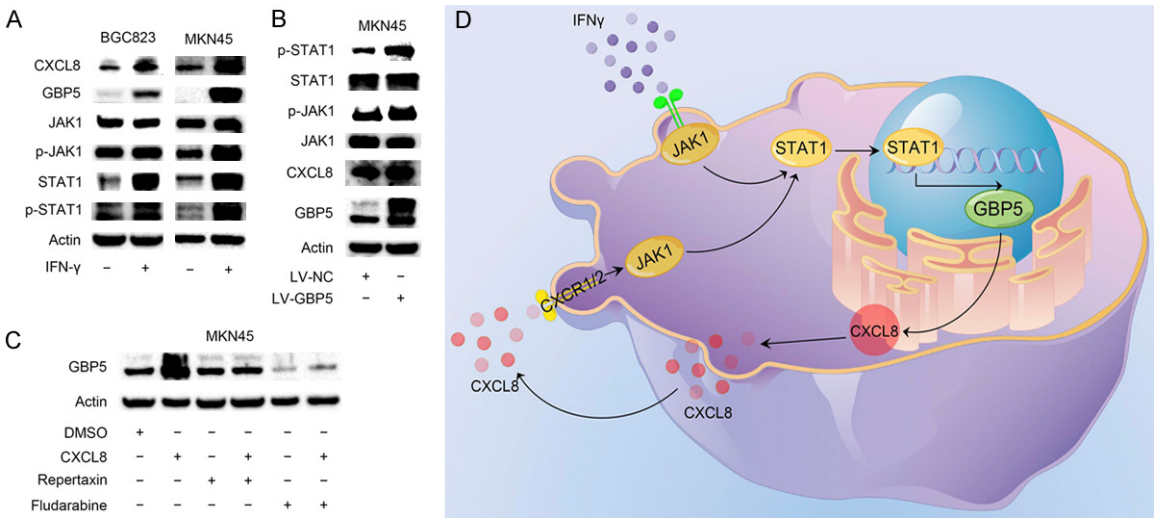

Figure 6. Reciprocal positive regulation between *GBP5* expression and *CXCL8-JAK1/STAT1* signaling. A. Effects of IFNγ treatment on STAT1, p-STAT1, JAK1, p-JAK1, GBP5, and CXCL8 levels in GC cells determined via western blotting. B. Effects of *GBP5* overexpression on CXCL8 expression and JAK1/STAT1 signaling pathway determined via western blotting. C. Protein levels of GBP5 in GC cells treated with CXCL8 with or without repertaxin/fludarabine determined via western blotting. D. Mechanism graph of the *JAK1-STAT1/GBP5/CXCL8* positive feedback loop.

CXCL8 has an impact on GBP5, we added CXCL8 alone or in combination with repertaxin (a CXCR1/2 small molecular inhibitor) or fludarabine to cells and detected GBP5 expression. Surprisingly, the addition of CXCL8 significantly increased the expression of GBP5, and GBP5 expression showed an apparent decrease when treated with Repertaxin or Fludarabine. Moreover, CXCL8 administration attenuated the fludarabine-induced decline in GBP5 expression (**Figure 6C**). Taken together, the above data verified the presence of a positive feedback loop between GBP5 and CXCL8 through the CXCL8-CXCR1 and JAK1/STAT1 signaling pathways (**Figure 6D**).

Association between GBP5 expression and TIME

Considering that GBPs are potential targets for immunotherapy [35], we next demonstrated the association between GBP5 and TIME in GC using bioinformatics methods. We divided GC samples in TCGA into hot and cold tumors based on the degree of CD8A expression, and found that GBP5 was significantly enriched in hot tumors, suggesting that GBP5 can predict a better immunotherapy response (**Figure 7A**). We also analyzed the association of some immune-related genes, including CD274, HLA-C, HLA-B, and HLA-A, with GBP5, and found a significant positive correlation between their mRNA expression (**Figure 7B**). In addition, we calculated the immune score, stroma score, tumor purity, and ESTIMATE score of the GC samples and compared their relationship with GBP5 (**Figure 7C**). The results showed that GBP5 was positively correlated with the immune, stromal, and ESTIMATE scores, and positively correlated with tumor purity. The degree of immune cell infiltration was determined using the CIBERSORT method. The fraction of CD8 T cells, CD4 memory activated T cells, follicular helper T cells, monocytes and macrophages M1 were higher in the GBP5 high expression group, and in the GBP5 low expression group, the fraction of CD4 memory resting T cells, regulatory T cells (Tregs), macrophages M0, mast cells, and eosinophils was lower (**Figure 7D**). Similar conclusions were obtained using the TIMER method. The expression of GBP5 was negatively correlated with tumor purity and B cell infiltration level and positively correlated with CD8+ T cells, CD4+ T cells, macrophages, neutrophils, and dendritic cell infiltration levels (**Figure 7E**). These results demonstrate the effect of GBP5 on the TIME in GC.

Discussion

GBPs induced by IFNγ have been shown to mediate antimicrobial responses, but the role of GBPs in cancer remains controversial [36].

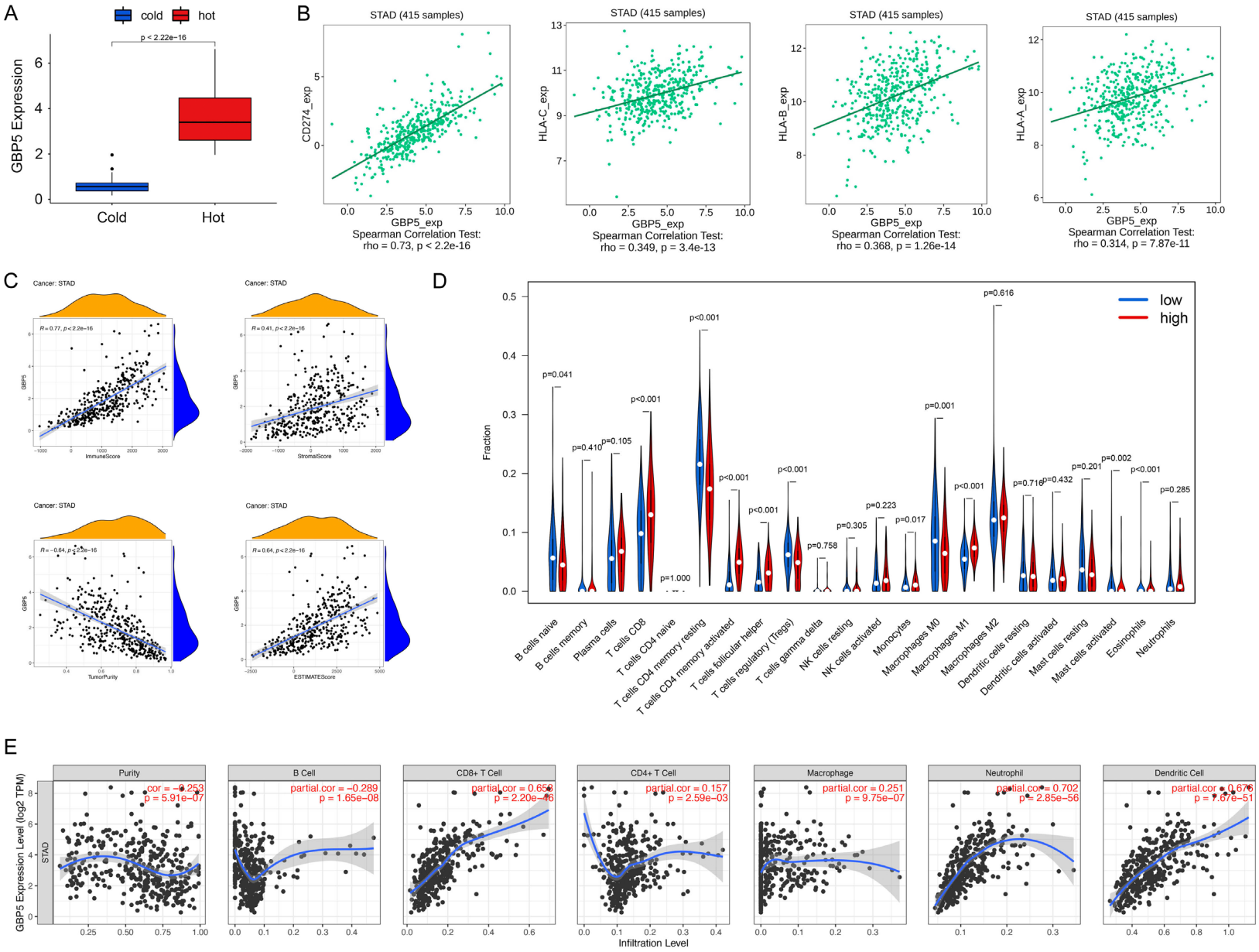
A
cold
hot
p < 2.22e−16
GBP5 Expression
Cold
Hot
B
STAD (415 samples)
CD274_exp
HLA-C_exp
HLA-B_exp
HLA-A_exp
GBP5_exp
Spearman Correlation Test:
rho = 0.73, p < 2.2e-16
rho = 0.349, p = 3.4e-13
rho = 0.368, p = 1.26e-14
rho = 0.314, p = 7.87e-11
C
Cancer: STAD
ImmuneScore
StromalScore
TumorPurity
ESTIMATEScore
D
low
high
Fraction
p=0.041
p=0.410
p=0.105
p<0.001
p=1.000
p=0.758
p=0.305
p=0.223
p=0.017
p=0.001
p=0.616
p=0.716
p=0.432
p=0.201
p=0.002
p=0.285
B cells naive
B cells memory
Plasma cells
T cells CD8
T cells CD4 naive
T cells CD4 memory resting
T cells CD4 memory activated
T cells follicular helper
T cells regulatory (Tregs)
T cells gamma delta
NK cells resting
NK cells activated
Monocytes
Macrophages M0
Macrophages M1
Macrophages M2
Dendritic cells resting
Dendritic cells activated
Mast cells resting
Mast cells activated
Eosinophils
Neutrophils
E
Purity
B Cell
CD8+ T Cell
CD4+ T Cell
Macrophage
Neutrophil
Dendritic Cell
GBP5 Expression Level (log2 TPM)
STAD
cor = −0.253
p = 5.91e−07
partial.cor = −0.289
p = 1.65e−08
partial.cor = 0.157
p = 2.59e−03
partial.cor = 0.251
p = 9.75e−07
partial.cor = 0.702
p = 2.85e−56
Infiltration Level

Figure 7. Correlation between *GBP5* expression and the tumor immune microenvironment (TIME) in GC. A. Differences in *GBP5* expression levels between hot and cold tumors in GC. B. Correlation between *GBP5* and immune-related gene expression levels. C. Correlation between *GBP5* expression and the Estimation of STromal and Immune cells in malignant Tumor tissues using Expression data (ESTIMATE) score. D. Differences in the fraction of tumor-infiltrating immune cells (TIICs) between GBP5-high and low expression groups in GC using the Cell-type Identification by Estimating Relative Subsets of RNA Transcripts (CIBERSORT). E. Correlation between GBP5 expression and the infiltration levels of TIICs using the Tumor Immune Estimation Resource (TIMER). Wilcoxon test was used for the significance test. $^{*}P < 0.05$, $^{**}P < 0.01$, and $^{***}P < 0.001$.

For example, GBP2 is associated with a better prognosis in bladder cancer, whereas the opposite is true in melanoma [37, 38]. As for GBP5, it is an oncogene in glioblastoma, oral squamous cell carcinoma, and triple-negative breast cancer [11-13]. However, the role of GBP5 in GC remains unclear. In this study, we found that GBP5 was highly expressed in tumor tissues and was associated with poor prognosis. We demonstrated that GBP5 could promote the proliferation and migration of gastric cancer cells in vitro. Mechanistically, GBP5 is regulated by the *IFNγ-JAK1-STAT1* signaling axis and promotes the malignant phenotype by inducing the expression of CXCL8, which can further activate the *JAK1-STAT1* signaling pathway to promote the expression of GBP5. In addition, GBP5 affected the tumor immune microenvironment. These results indicate that GBP5 is a potential target for molecular-targeted therapy and immunotherapy in GC.

IFNγ is a cytokine that can be used in antitumor therapy and often acts by activating the *JAK1-STAT1* signaling pathway [39]. However, owing to the serious side effects of IFNγ, it is still very important to study new targets in the IFNγ pathway. GBP5 has been shown to be regulated by IFNγ in autoimmune and inflammatory diseases as well as breast cancer [5, 12]. We found that GBP5 is similarly regulated by the *IFNγ-JAK1-STAT1* signaling axis in GC. In addition, we performed enrichment analysis of RNA-seq transcriptome data and found that multiple IFNγ-related pathways were enriched in GBP5 overexpressing cell lines. Our results suggest that IFNγ regulates GC cell proliferation and migration by inducing GBP5 expression, which is beneficial for the clinical application of IFNγ.

CXCL8, also known as interleukin-8, is a mediator of inflammation. Recent studies have shown that CXCL8 is secreted by tumor cells and mediates the malignant phenotype of tumors [40, 41]. CXCL8 promotes tumor metastasis and induces immune escape in GC [34, 42]. In this study, CXCL8 was one of the most significantly upregulated mRNAs in GBP5 overexpressing cell lines. We confirmed that GBP5 could regulate CXCL8 expression in vitro. Interestingly, CXCL8 affects GBP5 expression, which may represent a novel positive feedback loop in GC. Positive feedback loops are ubiquitous in tumors and closely related to tumor development [43]. Our results indicated that CXCL8 acting on the CXCR1 receptor can activate the *JAK1-STAT1* signaling pathway, which in turn induces GBP5 expression. Therefore, a positive feedback loop between GBP5 and CXCL8 may regulate GC progression.

Next, we explored the relationship between GBP5 and the TIME. Recent studies have shown that GBP1 has the potential to predict the effect of immunotherapy, but the effect of GBP5 on immunotherapy remains unknown [44]. Thus, TIME was classified into hot and cold tumors according to the degree of CD8+ T cell infiltration. GBP5 expression was significantly upregulated in hot tumors, which correlated with better immunotherapy efficacy. In addition, GBP5 was positively correlated with multiple immune-related genes, including PD-L1, and immune scores. Using different algorithms, we demonstrated that the abundance of CD8+ T cells was higher in the GBP5 high-expression group. These results partially explained the immunogenicity of GBP5. However, the correlation between GBP5 and TIME, as well as immunotherapy needs to be confirmed through functional experiments.

This study has some limitations. First, the results of RNA-seq and bioinformatics analyses were not verified in vivo. As GC tumors are complex ecosystems composed of different types of immune cells, the roles of *GBP5* within the TIME need to be further investigated. The lack of tumor-specific tumor microenvironment composition in most public datasets limited the clinical interpretation of *GBP5* function mecha-

nism. Thus, further experiments are needed to identify the interactions between *GBP5* and these cells in vivo to determine the anticancer immune response in the host. Here, we confirmed that *GBP5* promotes GC cell proliferation via a *GBP5/CXCL8* positive feedback loop in vitro. Whether disturbing this positive feedback loop using a specific inhibitor can promote the anticancer immune response remains unknown. Whether this finding can be transformed to benefit other targeted immunotherapies also remains unclear. A more detailed investigation of the mechanism of *GBP5* in cancer immunotherapy should be conducted at pre-clinical and clinical levels.

In conclusion, we revealed the biological functions of *GBP5* in GC in this study. *GBP5* is highly expressed in tumor tissues and is associated with poor prognosis of patients with GC. *GBP5* expression was regulated by the *IFNγ-JAK1-STAT1* signaling axis and promoted tumor cell proliferation and invasion by inducing the expression of *CXCL8*. Interestingly, CXCL8 further promoted *GBP5* expression by activating the *JAK1-STAT1* signaling pathway to form a new positive feedback loop. Moreover, *GBP5* expression was closely related to the TIME. Therefore, *GBP5* is a potential therapeutic target for GC.

Acknowledgements

We acknowledge the support from the lab team of the Department of Gastrointestinal Surgery and the Key Laboratory of Hubei Province for Digestive System Disease at Renmin Hospital of Wuhan University for their excellent clinical and experimental work. The Medical Ethics Committee of Renmin Hospital of Wuhan University and the Xijing Hospital's Protection of Human Subjects Committee approved the study. The study was supported by the Fundamental Research Funds for the Central Universities (2042022kf1089); the National Natural Science Foundation of China (grant number 82203713, 82100680); Chenxiaoping foundation for the development of science and technology of Hubei province (CXPJJH121003-2103).

Disclosure of conflict of interest

None.

Abbreviations

GC, Gastric cancer; GBP5, Guanylate binding protein 5; TIME, tumor immune microenvironment; IHC, immunohistochemistry; TMA, Tissue microarray; WB, Western Blotting; DAB, diaminobenzidine tetrahydrochloride; KEGG, Kyoto Encyclopedia of Genes and Genomes; GO, Gene Ontology; PPI, protein-to-protein interaction; GEPIA, Gene Expression Profiling Interactive Analysis; cBioPortal, cBio Cancer Genomics Portal; SRCC, signet-ring cell carcinoma; PDAC, Poorly Differentiated Adenocarcinoma; WMDAC, Well Moderately Differentiated Adenocarcinoma.

Address correspondence to: Dr. Dan Song and Yong-Bin Zheng, Department of Gastrointestinal Surgery, Key Laboratory of Hubei Province for Digestive System Disease, Renmin Hospital of Wuhan University, No. 99, Zhangzhidong Road, Wuchang District, Wuhan 430000, Hubei, China. Tel: +86-15826706525; E-mail: dansong@whu.edu.cn (DS); Tel: +86-13871189698; E-mail: yongbinzheng@whu.edu.cn (YBZ); Dr. Song Su, Department of Gastroenterology, The First Medical Center of Chinese PLA General Hospital, No. 28 Fuxing Road, Haidian District, Beijing 100853, China. Tel: +86-13439710906; E-mail: sssusong0808@126.com

References

[1] Siegel RL, Miller KD, Fuchs HE and Jemal A. Cancer statistics, 2022. CA Cancer J Clin 2022; 72: 7-33.

[2] Lyons K, Le LC, Pham YT, Borron C, Park JY, Tran CTD, Tran TV, Tran HT, Vu KT, Do CD, Pelucchi C, La Vecchia C, Zgibor J, Boffetta P and Luu HN. Gastric cancer: epidemiology, biology, and prevention: a mini review. Eur J Cancer Prev 2019; 28: 397-412.

[3] Xia C, Dong X, Li H, Cao M, Sun D, He S, Yang F, Yan X, Zhang S, Li N and Chen W. Cancer statistics in China and United States, 2022: profiles, trends, and determinants. Chin Med J (Engl) 2022; 135: 584-590.

[4] Matsuoka T and Yashiro M. Precision medicine for gastrointestinal cancer: recent progress and future perspective. World J Gastrointest Oncol 2020; 12: 1-20.

[5] Haque M, Siegel RJ, Fox DA and Ahmed S. Interferon-stimulated GTPases in autoimmune and inflammatory diseases: promising role for the guanylate-binding protein (GBP) family. Rheumatology (Oxford) 2021; 60: 494-506.

[6] Praefcke GJ and McMahon HT. The dynamin superfamily: universal membrane tubulation and fission molecules? Nat Rev Mol Cell Biol 2004; 5: 133-147.
[7] Martens S and Howard J. The interferon-inducible GTPases. Annu Rev Cell Dev Biol 2006; 22: 559-589.
[8] Kutsch M and Coers J. Human guanylate binding proteins: nanomachines orchestrating host defense. FEBS J 2021; 288: 5826-5849.
[9] Shenoy AR, Wellington DA, Kumar P, Kassa H, Booth CJ, Cresswell P and MacMicking JD. GBP5 promotes NLRP3 inflammasome assembly and immunity in mammals. Science 2012; 336: 481-485.
[10] Li G, Kryczek I, Nam J, Li X, Li S, Li J, Wei S, Grove S, Vatan L, Zhou J, Du W, Lin H, Wang T, Subramanian C, Moon JJ, Cieslik M, Cohen M and Zou W. LIMIT is an immunogenic lncRNA in cancer immunity and immunotherapy. Nat Cell Biol 2021; 23: 526-537.
[11] Yu X, Jin J, Zheng Y, Zhu H, Xu H, Ma J, Lan Q, Zhuang Z, Chen CC and Li M. GBP5 drives malignancy of glioblastoma via the Src/ERK1/2/MMP3 pathway. Cell Death Dis 2021; 12: 203.
[12] Cheng SW, Chen PC, Lin MH, Ger TR, Chiu HW and Lin YF. GBP5 repression suppresses the metastatic potential and PD-L1 expression in triple-negative breast cancer. Biomedicines 2021; 9: 371.
[13] Liu PF, Shu CW, Lee CH, Sie HC, Liou HH, Cheng JT, Ger LP, Chen CL, Chen CC and Chen CF. Clinical significance and the role of guanylate-binding protein 5 in oral squamous cell carcinoma. Cancers (Basel) 2021; 13: 4043.
[14] Friedman K, Brodsky AS, Lu S, Wood S, Gill AJ, Lombardo K, Yang D and Resnick MB. Medullary carcinoma of the colon: a distinct morphology reveals a distinctive immunoregulatory microenvironment. Mod Pathol 2016; 29: 528-541.
[15] Patil PA, Blakely AM, Lombardo KA, Machan JT, Miner TJ, Wang LJ, Marwaha AS and Matoso A. Expression of PD-L1, indoleamine 2,3-dioxygenase and the immune microenvironment in gastric adenocarcinoma. Histopathology 2018; 73: 124-136.
[16] Xiong X, Liao X, Qiu S, Xu H, Zhang S, Wang S, Ai J and Yang L. CXCL8 in tumor biology and its implications for clinical translation. Front Mol Biosci 2022; 9: 723846.
[17] Fousek K, Horn LA and Palena C. Interleukin-8: a chemokine at the intersection of cancer plasticity, angiogenesis, and immune suppression. Pharmacol Ther 2021; 219: 107692.
[18] Palombo R, Passacantilli I, Terracciano F, Capone A, Matteocci A, Tournier S, Alberdi A, Chiurchiù V, Volpe E and Paronetto MP. Inhibition of the PI3K/AKT/mTOR signaling promotes an M1 macrophage switch by repressing the ATF3-CXCL8 axis in Ewing sarcoma. Cancer Lett 2023; 555: 216042.
[19] Yang M, Zhang G, Wang Y, He M, Xu Q, Lu J, Liu H and Xu C. Tumour-associated neutrophils orchestrate intratumoural IL-8-driven immune evasion through Jagged2 activation in ovarian cancer. Br J Cancer 2020; 123: 1404-1416.
[20] Walle T, Kraske JA, Liao B, Lenoir B, Timke C, von Bohlen Und Halbach E, Tran F, Griebel P, Albrecht D, Ahmed A, Suarez-Carmona M, Jiménez-Sánchez A, Beikert T, Tietz-Dahlfuß A, Menevse AN, Schmidt G, Brom M, Pahl JHW, Antonopoulos W, Miller M, Perez RL, Bestvater F, Giese NA, Beckhove P, Rosenstiel P, Jäger D, Strobel O, Pe'er D, Halama N, Debus J, Cerwenka A and Huber PE. Radiotherapy orchestrates natural killer cell dependent antitumor immune responses through CXCL8. Sci Adv 2022; 8: eabh4050.
[21] Li E, Yang X, Du Y, Wang G, Chan DW, Wu D, Xu P, Ni P, Xu D and Hu Y. CXCL8 associated dendritic cell activation marker expression and recruitment as indicators of favorable outcomes in colorectal cancer. Front Immunol 2021; 12: 667177.
[22] Yuen KC, Liu LF, Gupta V, Madireddi S, Keerthivasan S, Li C, Rishipathak D, Williams P, Kadel EE 3rd, Koeppen H, Chen YJ, Modrusan Z, Grogan JL, Banchereau R, Leng N, Thastrom A, Shen X, Hashimoto K, Tayama D, van der Heijden MS, Rosenberg JE, McDermott DF, Powles T, Hegde PS, Huseni MA and Mariathasan S. High systemic and tumor-associated IL-8 correlates with reduced clinical benefit of PD-L1 blockade. Nat Med 2019; 26: 693-698.
[23] Schalper KA, Carleton M, Zhou M, Chen T, Feng Y, Huang SP, Walsh AM, Baxi V, Pandya D, Baradet T, Locke D, Wu Q, Reilly TP, Phillips P, Nagineni V, Gianino N, Gu J, Zhao H, Perez-Gracia JL, Sanmamed MF and Melero I. Elevated serum interleukin-8 is associated with enhanced intratumor neutrophils and reduced clinical benefit of immune-checkpoint inhibitors. Nat Med 2019; 26: 688-692.
[24] Shen Y, Zhang B, Wei X, Guan X and Zhang W. CXCL8 is a prognostic biomarker and correlated with TNBC brain metastasis and immune infiltration. Int Immunopharmacol 2022; 103: 108454.
[25] An R, Meng S and Qian H. Identification of key pathways and establishment of a seven-gene prognostic signature in cervical cancer. J Oncol 2022; 2022: 4748796.
[26] Ma Y, Wang B, He P, Qi W, Xiang L, Maswikiti EP and Chen H. Coagulation- and fibrinolysis-related genes for predicting survival and immunotherapy efficacy in colorectal cancer. Front Immunol 2022; 13: 1023908.

[27] Song D, Guo M, Xu S, Song X, Bai B, Li Z, Chen J, An Y, Nie Y, Wu K, Wang S and Zhao Q. HSP90-dependent PUS7 overexpression facilitates the metastasis of colorectal cancer cells by regulating LASP1 abundance. J Exp Clin Cancer Res 2021; 40: 170.
[28] Newman AM, Liu CL, Green MR, Gentles AJ, Feng W, Xu Y, Hoang CD, Diehn M and Alizadeh AA. Robust enumeration of cell subsets from tissue expression profiles. Nat Methods 2015; 12: 453-457.
[29] Li B, Severson E, Pignon JC, Zhao H, Li T, Novak J, Jiang P, Shen H, Aster JC, Rodig S, Signoretti S, Liu JS and Liu XS. Comprehensive analyses of tumor immunity: implications for cancer immunotherapy. Genome Biol 2016; 17: 174.
[30] Tang Z, Li C, Kang B, Gao G, Li C and Zhang Z. GEPIA: a web server for cancer and normal gene expression profiling and interactive analyses. Nucleic Acids Res 2017; 45: W98-W102.
[31] Lánczky A and Győrffy B. Web-based survival analysis tool tailored for medical research (KMplot): development and implementation. J Med Internet Res 2021; 23: e27633.
[32] Cerami E, Gao J, Dogrusoz U, Gross BE, Sumer SO, Aksoy BA, Jacobsen A, Byrne CJ, Heuer ML, Larsson E, Antipin Y, Reva B, Goldberg AP, Sander C and Schultz N. The cBio cancer genomics portal: an open platform for exploring multidimensional cancer genomics data. Cancer Discov 2012; 2: 401-404.
[33] Fan Y, Bai B, Liang Y, Ren Y, Liu Y, Zhou F, Lou X, Zi J, Hou G, Chen F, Zhao Q and Liu S. Proteomic profiling of gastric signet ring cell carcinoma tissues reveals characteristic changes of the complement cascade pathway. Mol Cell Proteomics 2021; 20: 100068.
[34] Lin C, He H, Liu H, Li R, Chen Y, Qi Y, Jiang Q, Chen L, Zhang P, Zhang H, Li H, Zhang W, Sun Y and Xu J. Tumour-associated macrophages-derived CXCL8 determines immune evasion through autonomous PD-L1 expression in gastric cancer. Gut 2019; 68: 1764-1773.
[35] Li X, Song D, Su S, He X, Cao F, Yang C, Li K, Huang S, Li C, Wang C, Zhang A, Pang P and Zheng Y. Critical role of guanylate binding protein 5 in tumor immune microenvironment and predictive value of immunotherapy response. Front Genet 2022; 13: 984615.
[36] Feng J, Cao Z, Wang L, Wan Y, Peng N, Wang Q, Chen X, Zhou Y and Zhu Y. Inducible GBP5 mediates the antiviral response via interferon-related pathways during influenza a virus infection. J Innate Immun 2017; 9: 419-435.
[37] Chen B, Sun D, Qin X and Gao XH. Screening and identification of potential biomarkers and therapeutic drugs in melanoma via integrated bioinformatics analysis. Invest New Drugs 2021; 39: 928-948.
[38] Wang L, Wang Y, Wang J, Li L and Bi J. Identification of a prognosis-related risk signature for bladder cancer to predict survival and immune landscapes. J Immunol Res 2021; 2021: 3236384.
[39] Zaidi MR and Merlino G. The two faces of interferon-γ in cancer. Clin Cancer Res 2011; 17: 6118-6124.
[40] Hsu YL, Hung JY, Ko YC, Hung CH, Huang MS and Kuo PL. Phospholipase D signaling pathway is involved in lung cancer-derived IL-8 increased osteoclastogenesis. Carcinogenesis 2010; 31: 587-596.
[41] Dominguez C, McCampbell KK, David JM and Palena C. Neutralization of IL-8 decreases tumor PMN-MDSCs and reduces mesenchymalization of claudin-low triple-negative breast cancer. JCI Insight 2017; 2: e94296.
[42] Chen L, Min L, Wang X, Zhao J, Chen H, Qin J, Chen W, Shen Z, Tang Z, Gan Q, Ruan Y, Sun Y, Qin X and Gu J. Loss of RACK1 promotes metastasis of gastric cancer by inducing a miR-302c/IL8 signaling loop. Cancer Res 2015; 75: 3832-3841.
[43] Yao H, Liu N, Lin MC and Zheng J. Positive feedback loop between cancer stem cells and angiogenesis in hepatocellular carcinoma. Cancer Lett 2016; 379: 213-219.
[44] Zhao Y, Wu J, Li L, Zhang H, Zhang H, Li J, Zhong H, Lei T, Jin Y, Xu B and Song Q. Guanylate-binding protein 1 as a potential predictor of immunotherapy: a pan-cancer analysis. Front Genet 2022; 13: 820135.